Int. J. Heat Mass Transfer. Vol. 32, No. 3, pp. 503–512, 1989
Printed in Great Britain

0017–9310/89 $3.00 + 0.00

The effective thermal conductivity for a point-contact porous medium: an experimental study

D. R. SHONNARD and S. WHITAKER
Department of Chemical Engineering, University of California, Davis, CA 95616, U.S.A.

(*Received* 9 *December* 1987 *and in final form* 28 *July* 1988)

Abstract—In order to test the inner expansion theory of Batchelor and O'Brien for a point-contact porous medium, a unit cell of a spatially periodic porous medium is constructed and used to measure the effective thermal conductivity. The unit cell is made of large, metal hemispheres which are brought into point-contact as determined by an abrupt change in the electrical conductivity of the system. Experimental data are obtained for ratios of the thermal conductivity k_σ/k_β ranging from 10^2 to 10^4 and the results verify the functional dependence of K_{eff} on k_σ/k_β predicted by Batchelor and O'Brien. In addition, our experimental data and the theory of Batchelor and O'Brien are in good agreement with the experimental results of Swift for metal powders having particle diameters of the order of hundreds of micrometers.

INTRODUCTION

FOR *passive* two-phase systems, such as we have illustrated in Fig. 1, one can measure the effective thermal conductivity with great accuracy [1] and produce results that are more reliable than those produced by current theories. Nevertheless, there is still considerable motivation to refine current theories, and to test theory and experiment with the objective of developing an improved understanding of the interaction between heat conduction and the complex geometries encountered in two-phase systems. Our motivation results largely from an interest in *active* systems, i.e. systems in which heterogeneous or homogeneous thermal sources exist owing to chemical reaction and phase change [2, 3]. The classic example is a three-phase system consisting of a solid, a liquid and a gas. When subject to a temperature gradient, evaporation and condensation can occur thus generating an additional transport mechanism in the gas phase, and liquid-phase transport can also occur owing to capillary forces. The simple experimental study for a two-phase system suddenly becomes extremely complex for a three-phase system, and for this reason a comprehensive understanding of the influence of geometry and k_σ/k_β on the effective thermal conductivity is desirable.

The process under consideration can be described by the following boundary value problem:

$$(\rho c_p)_\beta \frac{\partial T_\beta}{\partial t} = \nabla \cdot (k_\beta \nabla T_\beta), \quad \beta\text{-phase} \tag{1}$$

B.C.1

$$T_\beta = T_\sigma, \quad \beta\text{–}\sigma \text{ interface} \tag{2}$$

B.C.2

$$\mathbf{n}_{\beta\sigma} \cdot k_\beta \nabla T_\beta = \mathbf{n}_{\beta\sigma} \cdot k_\sigma \nabla T_\sigma, \quad \beta\text{–}\sigma \text{ interface} \tag{3}$$

$$(\rho c_p)_\sigma \frac{\partial T_\sigma}{\partial t} = \nabla \cdot (k_\sigma \nabla T_\sigma), \quad \sigma\text{-phase} \tag{4}$$

B.C.3

$$T_\beta = f(t), \quad \text{at } \mathscr{A}_{\beta e} \tag{5}$$

B.C.4

$$T_\sigma = g(t), \quad \text{at } \mathscr{A}_{\sigma e}. \tag{6}$$

Here $\mathscr{A}_{\beta e}$ and $\mathscr{A}_{\sigma e}$ represent the areas of the entrances and exits for the macroscopic system illustrated in Fig. 2, and in general the boundary conditions at $\mathscr{A}_{\beta e}$ and $\mathscr{A}_{\sigma e}$ are known only in terms of *average temperatures* rather than the point temperatures T_β and T_σ.

In our approach to this problem we assume that it is sufficient to determine an average temperature associated with the averaging volume, $\mathscr{V}$, illustrated in Fig. 2 and shown in detail in Fig. 3. For the β-phase contained in the averaging volume, we define an

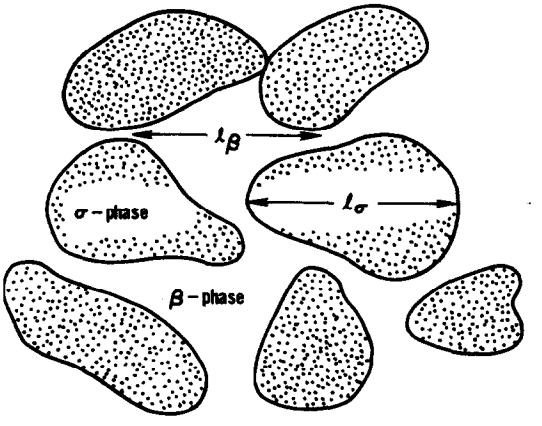

FIG. 1. Rigid, two-phase system.

NOMENCLATURE

$A_{\beta\sigma}$ area of the β–σ interface contained within the averaging volume [m^2]
$(c_p)_\omega$ constant pressure heat capacity for the ω-phase [kcal kg^{-1} K^{-1}]
C_p mass fraction weighted heat capacity [kcal kg^{-1} K^{-1}]
D diameter [m]
$\mathbf{f}$ vector field that maps $\nabla\langle T_\beta\rangle^\beta$ onto $T_\beta - \langle T_\beta\rangle^\beta$ [m]
$\mathbf{g}$ vector field that maps $\nabla\langle T_\sigma\rangle^\sigma$ onto $T_\sigma - \langle T_\sigma\rangle^\sigma$ [m]
k_{ref} thermal conductivity of the reference material [kcal m^{-1} s^{-1} K^{-1}]
k_ω thermal conductivity for the ω-phase [kcal m^{-1} s^{-1} K^{-1}]
$\underline{\mathbf{K}}_{\text{eff}}$ effective thermal conductivity tensor [kcal m^{-1} s^{-1} K^{-1}]
L length [m]
$\mathbf{n}_{\beta\sigma}$ outwardly directed unit normal pointing from the β-phase toward the σ-phase, $-\mathbf{n}_{\sigma\beta}$
T_ω point temperature in the ω-phase [K]
$\langle T_\omega\rangle^\omega$ intrinsic phase averaged temperature in the ω-phase [K]
$\tilde{T}_\omega$ spatial deviation temperature in the ω-phase, $T_\omega - \langle T_\omega\rangle^\omega$
$\langle T\rangle$ spatial average temperature, $\varepsilon_\beta\langle T_\beta\rangle^\beta + \varepsilon_\sigma\langle T_\sigma\rangle^\sigma$ [K]
$\mathcal{V}$ averaging volume [m^3].

Greek symbols

βe area of entrances and exits for the β-phase [m^2]
σe area of entrances and exits for the σ-phase [m^2].

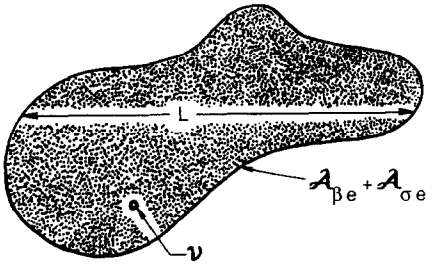

FIG. 2. Macroscopic domain.

intrinsic phase averaged temperature by

$$\langle T_\beta\rangle^\beta = \frac{1}{V_\beta}\int_{V_\beta} T_\beta \, dV \tag{7}$$

and a spatial deviation temperature $\tilde{T}_\beta$ according to

$$T_\beta = \langle T_\beta\rangle^\beta + \tilde{T}_\beta. \tag{8}$$

With these definitions, the method of volume averaging [4, 5] leads to the following equation for the β-phase:

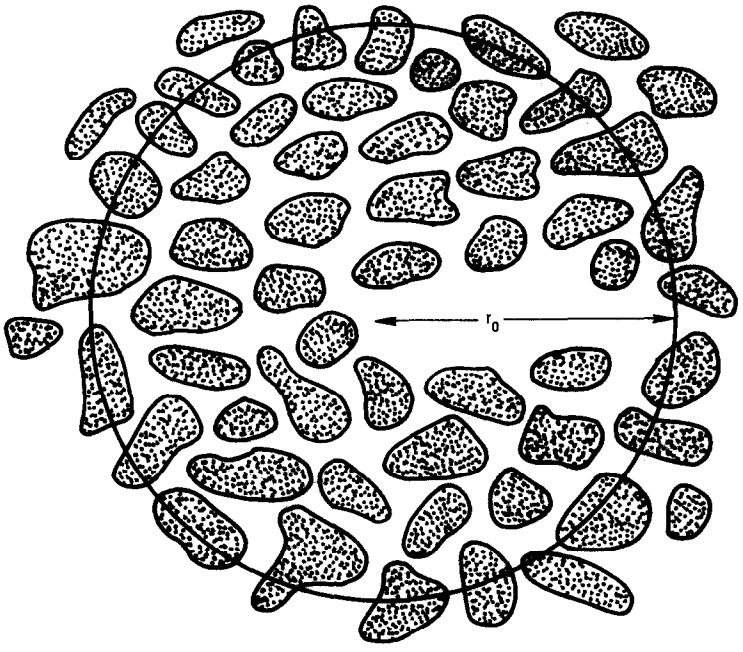

FIG. 3. Averaging volume.

$$\varepsilon_\beta(\rho c_p)_\beta \frac{\partial \langle T_\beta \rangle^\beta}{\partial t} = \nabla \cdot \left[\varepsilon_\beta k_\beta \nabla \langle T_\beta \rangle^\beta + \frac{1}{V_\beta} \int_{A_{\beta\sigma}} \mathbf{n}_{\beta\sigma} \tilde{T}_\beta \, dA \right] + \frac{1}{\mathscr{V}} \int_{A_{\beta\sigma}} \mathbf{n}_{\beta\sigma} \cdot k_\beta \nabla T_\beta \, dA. \quad (9)$$

Here ε_β represents the volume fraction of the β-phase and is given explicitly by

$$\varepsilon_\beta = V_\beta / \mathscr{V}. \quad (10)$$

In equation (9) it should be clear that the first term represents the accumulation of energy in the β-phase, the second term represents the conductive transport in the β-phase, and the last term represents the heat transfer between the β-phase and the σ-phase within the averaging volume.

For the σ-phase, one begins with equation (4) in order to arrive at an equation analogous to equation (9)

$$\varepsilon_\sigma(\rho c_p)_\sigma \frac{\partial \langle T_\sigma \rangle^\sigma}{\partial t} = \nabla \cdot \left[\varepsilon_\sigma k_\sigma \nabla \langle T_\sigma \rangle^\sigma + \frac{1}{V_\sigma} \int_{A_{\beta\sigma}} \mathbf{n}_{\sigma\beta} \tilde{T}_\sigma \, dA \right] + \frac{1}{\mathscr{V}} \int_{A_{\beta\sigma}} \mathbf{n}_{\sigma\beta} \cdot k_\sigma \nabla T_\sigma \, dA. \quad (11)$$

When the condition of local thermal equilibrium prevails [2, 6], the two temperatures, $\langle T_\beta \rangle^\beta$ and $\langle T_\sigma \rangle^\sigma$, are sufficiently close so that the thermal process can be accurately represented by a *single temperature*. This is the spatial average temperature given by

$$\langle T \rangle = \varepsilon_\beta \langle T_\beta \rangle^\beta + \varepsilon_\sigma \langle T_\sigma \rangle^\sigma. \quad (12)$$

Under these circumstances equations (9) and (11) can be added in order to obtain

$$\langle \rho \rangle C_p \frac{\partial \langle T \rangle}{\partial t} = \nabla \cdot [(\varepsilon_\beta k_\beta + \varepsilon_\sigma k_\sigma) \underline{\mathbf{I}}] \cdot \nabla \langle T \rangle + \frac{k_\beta}{\mathscr{V}} \int_{A_{\beta\sigma}} \mathbf{n}_{\beta\sigma} \tilde{T}_\beta \, dA + \frac{k_\sigma}{\mathscr{V}} \int_{A_{\beta\sigma}} \mathbf{n}_{\sigma\beta} \tilde{T}_\sigma \, dA. \quad (13)$$

The closure problem is described by Nozad *et al.* [5] and it indicates that $\tilde{T}_\beta$ and $\tilde{T}_\sigma$ are given by

$$\tilde{T}_\beta = \mathbf{f} \cdot \nabla \langle T \rangle, \quad \tilde{T}_\sigma = \mathbf{g} \cdot \nabla \langle T \rangle \quad (14)$$

where the vector fields are determined in a unit cell of a spatially periodic porous medium [7] according to the following boundary value problem:

$$\nabla^2 \mathbf{f} = 0, \quad \beta\text{-phase} \quad (15)$$

B.C.1

$$\mathbf{f} = \mathbf{g}, \quad \beta\text{–}\sigma \text{ interface} \quad (16)$$

B.C.2

$$\mathbf{n}_{\beta\sigma} \cdot k_\beta \nabla \mathbf{f} = \mathbf{n}_{\beta\sigma} \cdot k_\sigma \nabla \mathbf{g} + \mathbf{n}_{\beta\sigma}(k_\sigma - k_\beta), \quad \beta\text{–}\sigma \text{ interface} \quad (17)$$

$$\nabla^2 \mathbf{g} = 0, \quad \sigma\text{-phase} \quad (18)$$

$$\mathbf{f}(\mathbf{r}+\mathbf{l}_i) = \mathbf{f}(\mathbf{r}), \quad \mathbf{g}(\mathbf{r}+\mathbf{l}_i) = \mathbf{g}(\mathbf{r}), \quad i = 1,2,3 \quad (19)$$

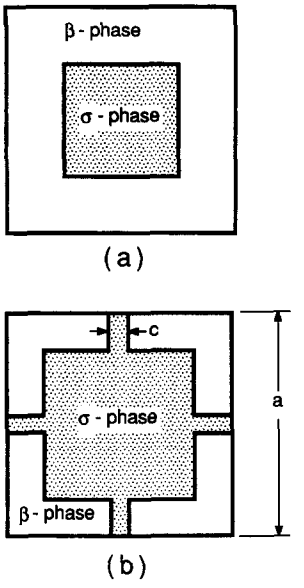

FIG. 4. Unit cells.

$$\langle \mathbf{f} \rangle^\beta = 0, \quad \langle \mathbf{g} \rangle^\sigma = 0. \quad (20)$$

Here $\mathbf{l}_i$ represents the three lattice vectors needed to describe a unit cell in a spatially periodic porous medium. Nozad *et al.* [5] have shown that the boundary conditions associated with the vector fields $\mathbf{f}$ and $\mathbf{g}$ can be used to derive the classic temperature conditions used in structural models [8–11]. We use the phrase *structural model* in the sense of Jiang *et al.* [12] in order to establish the difference between the boundary value problem associated with the primitive variable and that associated with the vector fields $\mathbf{f}$ and $\mathbf{g}$. In general, the closure problem as given by equations (15)–(20) is analogous to what one would obtain using the method of spatial homogenization [13, 14].

When equations (14) are used in equation (13) we obtain

$$\langle \rho \rangle C_p \frac{\partial \langle T \rangle}{\partial t} = \nabla \cdot (\underline{\mathbf{K}}_{\text{eff}} \cdot \nabla \langle T \rangle) \quad (21)$$

and it is convenient to represent the dimensionless effective thermal conductivity tensor as

$$\frac{\underline{\mathbf{K}}_{\text{eff}}}{k_\beta} = (\varepsilon_\beta + \kappa \varepsilon_\sigma) \underline{\mathbf{I}} + \frac{(1-\kappa)}{\mathscr{V}} \int_{A_{\beta\sigma}} \mathbf{n}_{\beta\sigma} \mathbf{f} \, dA. \quad (22)$$

Here we have used κ to represent the ratio of conductivities according to

$$\kappa = k_\sigma / k_\beta. \quad (23)$$

From the closure problem given by equations (15)–(20) and (22), it should be clear that the dimensionless effective thermal conductivity tensor, $\underline{\mathbf{K}}_{\text{eff}}/k_\beta$, will be a function of the ratio of thermal conductivities, κ, the volume fraction of the β-phase, $\varepsilon_\beta = 1 - \varepsilon_\sigma$, and the geometry of the system as given by $\mathbf{n}_{\beta\sigma}$ in equation (17).

The closure problem has been solved by Nozad *et al.* [5] for the unit cells indicated in Fig. 4, and for

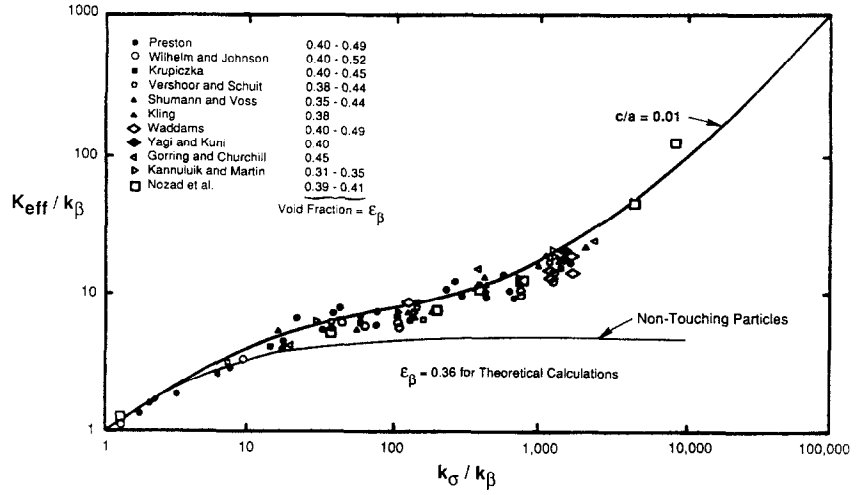

FIG. 5. Comparison between theory and experiment.

these types of systems the thermal conductivity tensor is isotropic. For large values of κ an *outer expansion* in the perturbation parameter, κ^{-1}, was used by Nozad *et al.* to solve equations (15)–(20) and the results of their solution are shown in Fig. 5. For large values of κ, the outer expansion indicates that K_{eff}/k_β is a linear function of κ when there is contact between the particles that make up the σ-phase.† When there is no contact between the particles that make up the σ-phase, the outer expansion for the closure problem indicates that K_{eff}/k_β is independent of κ. The scatter in the data shown in Fig. 5 is due largely to the variations of the volume fraction, and if one considers the comparison presented by Nozad *et al.* [5] for a very narrow range of values of ε_β one finds extremely good agreement between theory and experiment. Because of this, and because of the reasonably good agreement between the experimental results and the single theoretical result for $c/a = 0.01$, one might be tempted to think of this particular value of c/a as representing a universal parameter for unconsolidated porous media.‡ *This would most certainly be a mistake.* In an unpublished study by Wu [18], the experimental equipment of Nozad [16] was re-used to measure the effective thermal conductivity for systems consisting of spheres of urea formaldehyde, stainless steel, bronze, glass and aluminum with air being the continuous fluid phase. All the experimental values for the effective thermal conductivity were in excellent agreement with those obtained by Nozad *except for* the aluminum–air system. The porous medium made from the 1 mm diameter aluminum spheres originally used by Nozad produced an effective thermal conductivity that was *four times larger* than that first measured by Nozad. An inspection of the spheres indicated that they had been deformed by use in other experiments performed in our laboratory and therefore produced a porous medium with a larger effective contact area between the solid particles. When Wu repeated the experiments with *new aluminum spheres*, the original results of Nozad were reproduced without difficulty. The conclusion here should be obvious: the effective thermal conductivity is very sensitive to the nature of the particle–particle contact at large values of the ratio, $\kappa = k_\sigma/k_\beta$. A dramatic example of this fact is contained in the theoretical study of Batchelor and O'Brien [19]. They considered a regular array of spheres which were in contact at *single points* as illustrated in Fig. 6. Their system is similar to that shown in Fig. 4(b) with the squares replaced by spheres and the contact area tending toward zero, i.e. $c/a \to 0$. Batchelor and O'Brien developed a solution for large values of κ in terms of an inner expansion and they represented their results as

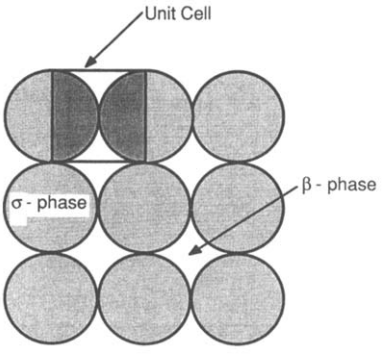

FIG. 6. Model for point-contact heat transfer.

† The linear dependence upon κ has also been obtained by Ogniewicz and Yovanovich [15]. This can be seen in their equation (20) and their calculations indicating that $I/L = \mathbf{0}(10)$ for small values of M. The nature of their result implies the use of an *outer expansion* in the solution of the particle–particle heat transfer problem.

‡ In the original work of Nozad [16] the value of $c/a = 0.02$ was used to produce the results shown in Fig. 5; however, an error in Nozad's calculations was subsequently detected and the calculations were repeated by Oppio [17] in order to obtain the value of 0.01.

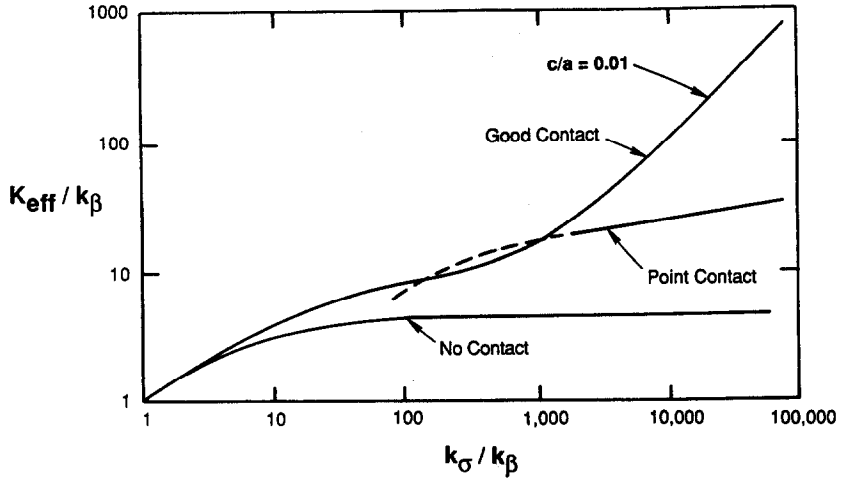

FIG. 7. Predicted effective thermal conductivity for good contact, point contact and poor contact.

$$\frac{K_{\text{eff}}}{k_\beta} = 4\ln(\kappa) - 11. \tag{24}$$

The number eleven in this expression represents an adjustable parameter which can only be determined precisely by matching the inner expansion with the outer expansion. The value of the adjustable parameter was chosen on the basis of experimental data with values of κ ranging from 30 to 3000, and equation (24) tended to *underpredict* the effective thermal conductivity for the large values of κ. The comparison of the analysis of Batchelor and O'Brien with the results of Nozad *et al.* is illustrated in Fig. 7. The outer expansion results have been identified as the *good contact* and the *no contact* results, while equation (24) has been identified as the *point-contact* result. From Fig. 7, two conclusions can be drawn:

(1) theoretical results are needed for the regions between the three curves;

(2) the inner expansion results differ dramatically from the outer expansion results for values of $\kappa \geqslant 10^4$.

In addition, one can conclude that the point-contact theory of Batchelor and O'Brien needs to be compared with experiment.

EXPERIMENTAL STUDIES

The unit cell that we wish to study from an experimental point of view is illustrated in Fig. 6, and a photograph of the experimental unit cell is shown in Fig. 8. In traditional studies of heat conduction in porous media [1] one utilizes relatively small particles in order to suppress the effects of radiation and natural convection, and the sample dimensions are chosen so that a one-dimensional heat flux is achieved. None of these traditional experimental precautions are available to us in this study of point-contact heat transfer between two hemispheres, thus we are faced with four experimental problems:

(1) the effect of radiation;

(2) the effect of natural convection;

(3) the difficulty of achieving a one-dimensional heat flux;

(4) the impossibility of achieving a point-contact system in the mathematical sense.

The first three problems were studied primarily from an experimental point of view, while the difference between the experimental solid–solid contact and the mathematical representation of a point-contact system was left as a site-specific characteristic of this study.

One can use a parallel plate, gray body model of conductive and radiative heat transfer to estimate the ratio of radiative transfer to conductive transfer as

$$\frac{\text{radiation}}{\text{conduction}} \sim \frac{4\sigma\varepsilon T_{\text{avg}}^3 D}{K_{\text{eff}}}. \tag{25}$$

Here ε represents the emissivity, and for the systems that we have studied ε is of the order of 0.10. Our measured values of K_{eff} were of the order of 1.0 W m^{-1} K^{-1} and T_{avg} was about 300 K. For a value of $D = 5$ cm one finds from equation (25) that

$$\frac{\text{radiation}}{\text{conduction}} \sim 0.03 \tag{26}$$

thus radiation can be neglected. When the characteristic length is of the order of 5 cm, one normally needs to be concerned about radiative transfer; however, in this study the values of k_σ (and therefore K_{eff}) were relatively large and this led to a situation in which conduction was large compared to radiation.

In most experimental studies of the thermal conductivity, one is free to arrange the geometry of the system so that a one-dimensional heat flux is obtained. In a study of heat conduction between hemispheres in point-contact, this is not possible and one is confronted with a serious problem of non-uniform heat

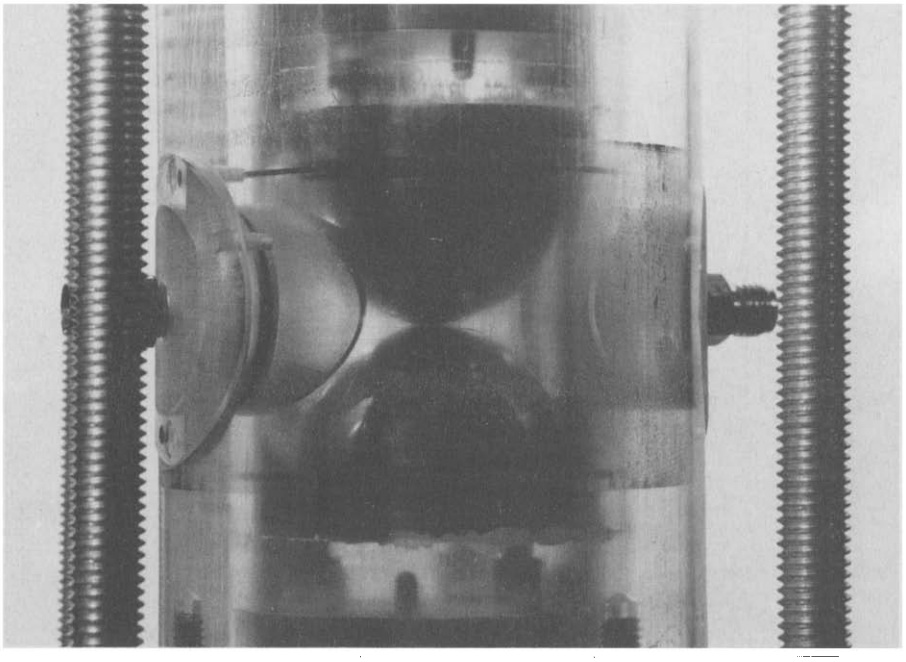

FIG. 8. Experimental unit cell.

flow. A schematic diagram of our experimental system is shown in Fig. 9. The unit cell is located in a plexiglass cylinder which provides the structural support for the system. If the thermal conductivity of plexiglass were *small* compared to the effective thermal conductivity of the unit cell, the plexiglass cylinder would act as an insulator which would give rise to a uniform heat flow in the thermal conductivity cell. Unfortunately the thermal conductivity of plexiglass is the same order as the measured effective thermal conductivities, and this creates a two-dimensional heat conduction process. We attempted to counteract this problem with the use of guard heaters and coolers, and we will describe our strategy in subsequent paragraphs.

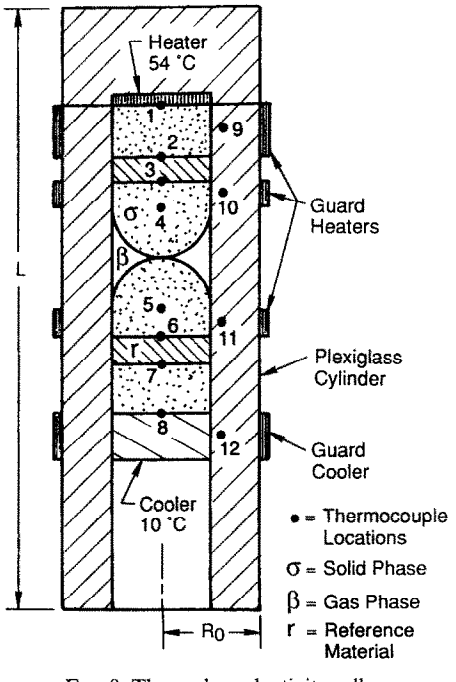

FIG. 9. Thermal conductivity cell.

In this experimental study, a steady-state comparative method was used. Energy is supplied at the top of the thermal conductivity cell by an electrical heater which causes a heat flow in a metal cylinder of the σ-phase just below the heater. The thermal conductivity of the σ-phase is several orders of magnitude larger than the disk of the comparative material, thus a uniform temperature exists on the upper surface of the disk and this is measured by thermocouple 2. The bottom surface of the disk of comparative material is also in contact with the σ-phase and therefore at a uniform temperature. This temperature is measured by thermocouple 3 and these two measurements are used to determine the heat flux at the top of the unit cell. A comparative disk is also placed at the bottom of the cell and the temperatures measured by thermocouples 6 and 7 allow us to calculate the heat flux at the bottom of the unit cell. In order to have a comparative material with nearly the same thermal conductivity as the unit cell, we used plexiglass for the comparative disks. This means that the disks had the same thermal conductivity as the surrounding material, and under these circumstances the assumption of one-dimensional heat conduction is not very attractive.

The temperature difference across the unit cell was determined by thermocouples 4 and 5, and knowledge of this temperature difference, the size of the unit cell, and the heat flux led to the experimental value of the

effective thermal conductivity. The traditional errors associated with temperature measurement and determination of the distance between thermocouples 4 and 5 are discussed by Shonnard [20]; however, those errors are small compared to the error associated with the lack of a one-dimensional heat conduction process. The heat flux in the unit cell was taken to be the average of the heat flux measured at the top of the cell and that measured at the bottom of the cell. These two values were usually within 3% of each other; however, that gives no indication of the absolute accuracy of the measurement nor does it guarantee that the heat flux in the unit cell is one-dimensional.

In an attempt to maintain a one-dimensional heat flux in the unit cell, guard heaters and coolers were placed around the system as indicated in Fig. 9. This configuration was based on the idea that radial heat conduction over the central portion of the cell would be negligible because of the low thermal conductivity of the gas in the cell. However, in the regions where the surrounding plexiglass wall is in contact with solid material we expect to find significant radial conduction. To determine the heater and cooler settings, thermocouples were placed in the plexiglass cylinder at the locations identified as 9, 10, 11 and 12 in Fig. 9. The position of these thermocouples was determined precisely so that the temperature measurements could be used in conjunction with a computer simulation. From a purely intuitive point of view, one might guess that the heater and cooler settings should be arranged to minimize the measured temperature differences between the outer surface of the plexiglass cylinder and the σ-phase in contact with the inner surface at the four locations. To provide guidance concerning the two-dimensional heat conduction process, a numerical solution of a model problem was developed.

COMPUTER SIMULATION

The system used to model the experimental apparatus shown in Fig. 9 was generated by replacing the unit cell with a homogeneous medium having a thermal conductivity equal to the effective thermal conductivity, K_{eff}. This system and the model boundary conditions are illustrated in Fig. 10. The regions associated with the boundary conditions identified by B.C.$_{\text{top}}$, B.C.1, B.C.2, and B.C.$_{\text{bot}}$ are regions where the surface temperature can be adjusted by the heaters and coolers. Those portions of the plexiglass that are in contact with the surrounding air are identified with the zero flux condition. The boundary condition at the center of the cell was arbitrarily specified as $\theta = 0.5$. While this is only correct if $\partial\theta/\partial r = 0$ at $r = R_0$, it allows for the computation time to be reduced by a factor of four and it is in keeping with the approximate nature of the simulation.

The results of the computer simulation were interpreted in terms of Q_{meas} (this is the average measured heat flux in the comparative disks) and Q_{cell} (this is the measured heat flux in the unit cell). By *measured* we mean determined in the same way as was done in the laboratory experiments. Three types of simulations were carried out.

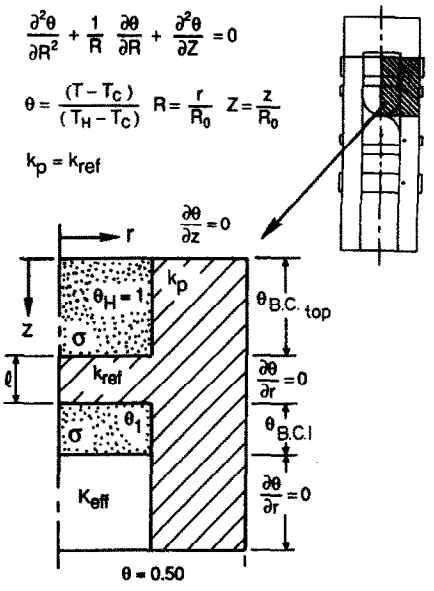

FIG. 10. Computer simulation of radial heat losses: model unit cell.

(1) The boundary conditions at the heaters and coolers were replaced with the zero flux condition. This is comparable to operating the equipment without the use of guard heaters or coolers and the results are identified as ERROR1 in Table 1.

(2) The boundary conditions at the heaters and coolers were set so that the temperatures were equal to the (essentially) uniform temperature in the σ-phase at the same position in the system. Most of our experimental data were taken under these conditions and the results are identified as ERROR2 in Table 1.

(3) The boundary conditions were adjusted (by trial and error) so that the difference between Q_{meas} and Q_{cell} was less than 5%. These results are identified as OPTIM in Table 1.

From these computed results we can see that the

Table 1. Results of computer simulation

Boundary conditions	$K_{\text{eff}}/k_{\text{ref}}$	l/R_0	$\frac{Q_{\text{meas}} - Q_{\text{cell}}}{Q_{\text{cell}}} \times 100$
ERROR1	5.0	0.125	−23.3
ERROR1	12.5	0.125	−32.6
ERROR1	1.0	0.25	20.0
ERROR1	2.5	0.25	−21.4
ERROR2	5.0	0.125	−12.6
ERROR2	12.5	0.125	−14.8
ERROR2	1.0	0.25	−6.7
ERROR2	2.5	0.25	−14.4
OPTIM	5.0	0.125	−4.3
OPTIM	12.5	0.125	−4.0
OPTIM	20.0	0.125	−4.2

l/R_0, dimensionless thickness of reference disk.

Table 2. Physical properties

Material		β (μm m^{-1} K^{-1})	c_p (J kg^{-1} K^{-1})	k (W m^{-1} K^{-1})
Aluminum	type 6061 T_6 temper 1% Mg, 0.6% Si 0.3% Cu, 0.2% Cr	23.6 c. 25°C	896	167.0
Stainless steel	type 303	17.2	500	16.2
Copper	type C11000	17.0	380 c. 20°C	387.0 c. 20°C
Plexiglass	(Polymethyl methacrylate)	4.0	1465	0.1955
Air	$\mu = 1.9 \times 10^{-5}$ N s m^{-2} at 37.5°C		1005	0.0264
Helium	$\mu = 1.8 \times 10^{-5}$ N s m^{-2} at 30°C		5192	0.1530
Air–fiberglass		—	—	0.0333
He–fiberglass		—	—	0.1580

β, thermal expansion coefficient.
c_p, heat capacity.
All composition values represent maximum values.

influence of two-dimensional heat conduction is significant, that operation of the heaters and coolers to generate a negligible radial temperature change provides an attractive improvement, and that an optimum routine that can reduce the error to a relatively low level may exist. The most important conclusion to be drawn from the computer simulation is the fact that we can expect errors of the order of 20% because of the non-uniform heat flux, and we should expect that the measured values of K_{eff} will be too small.

EXPERIMENTAL RESULTS

In all the experimental runs, the disk-shaped electric heater located at the top of the system was maintained at 54°C while the bottom of the system was maintained at 10°C by cooling water. This led to an average temperature of 32°C. The physical properties of the materials used in our experiments are listed in Table 2, and the thermal conductivities for the gas–fiberglass systems are based on the experimental studies of Fournier and Klarsfeld [21].

One can estimate a Rayleigh number for the unit cell [20], and for air this is about 10^4 while helium produces a value of about 700. From the experimental studies of Powe *et al.* [22] one is led to believe that natural convection may increase the 'effective' thermal conductivity of air by almost a factor of two while the effect for helium is negligible. Our experimental treatment of the problem of natural convection consisted of carrying out experiments with air and helium, both with and without fiberglass insulation. The influence of natural convection is shown in terms of the experimental values of K_{eff}/k_β presented in Fig. 11. In the absence of any fiberglass to suppress the natural convection, we see that the experimental values for air are more than twice as large as the values that one would expect to find for helium at a comparable value of κ. This is consistent with the estimated Rayleigh number and the experimental studies of Powe *et al.* [22]. The results using fiberglass to suppress the natural convection all lie below the results for pure air, as one would expect. In addition, the results using fiberglass are generally higher than the values for pure helium. This may be caused by a change in the nature of the contact between the two hemispheres when some strands of fiberglass are present. Clearly there is considerable scatter in the experimental data, and one must keep in mind that the log–log scale tends to hide this error.

The original experimental results are listed in Table 3 along with the experimental run time in hours. The characteristic time for the experimental system was about 6 h; however, the heater/cooler adjustments were all made manually. This often led to run times of 2 days and when experiments of this type are carried out under changing laboratory conditions one should expect to find significant errors. Three experimental runs were made using the optimum heater/cooling settings as determined by the computer simulation. These all gave higher experimental values as illustrated in Fig. 12. From this we conclude that the numerical simulator can provide some useful qualitative information about the influence of a non-uniform heat flux.

In Fig. 13 we have shown the comparison between our experimental results for gas–fiber systems, the

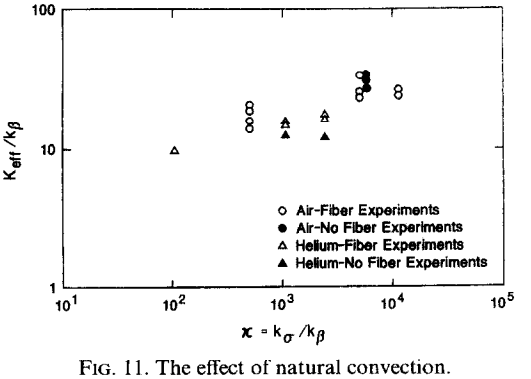

FIG. 11. The effect of natural convection.

Table 3. Experimental data

κ	K_{eff}/k_β	System	Run time (h)
5759	31.6	Al–air	33
5759	27.7	Al–air	48
11 610	24.5	Cu–air–fiber	42
11 610	26.9	Cu–air–fiber	58
485	20.9	SS–air–fiber	—
485	18.8	SS–air–fiber	—
485	14.3	SS–air–fiber	60
485	16.0	SS–air–fiber	20
5010	23.5	Al–air–fiber	71
5010	34.6	Al–air–fiber	45
1057	16.0	Al–He–fiber	32
1057	16.2	Al–He–fiber	47
1092	12.9	Al–He	29
1057	14.9	Al–He–fiber	38
5010	26.0	Al–air–fiber	24
5759	34.7	Al–air	44
2529	12.6	Cu–He	20
2449	16.6	Cu–He–fiber	29
2449	17.8	Cu–He–fiber	39
2449	24.4	Cu–He–fiber	38 (optimum)
2449	20.8	Cu–He–fiber	30 (optimum)
101	9.94	SS–He–fiber	34
101	12.6	SS–He–fiber	22 (optimum)
485	21.4	SS–air–fiber	52

theory of Batchelor and O'Brien [19] as given by equation (24), and the experimental data of Swift [23]. The comparison with the theory of Batchelor and O'Brien is reasonably good, and certainly tends to confirm the logarithmic dependence on κ. What is surprising is the similarity between experimental results for large hemispheres brought into point contact with results for packed metal powders for which the particle diameter is of the order of hundreds of micrometers. This, of course, must also be contrasted with the results of Nozad shown in Fig. 5 for spherical particles having diameters of the order of 2 mm. The data of Swift shown in Fig. 13 were all obtained at gas pressures that were high enough so that the measured effective thermal conductivity was independent of pressure. Under these circumstances free molecule transport effects can be ignored and Swift's results should be consistent with the equations and boundary conditions given by equations (1)–(6). That a packed powder of 100 μm diameter spherical metal particles would behave in the same manner as 5 cm diameter metal hemispheres brought into point contact is a curious situation. However, Swift's experiments were performed with great care for a wide variety of gas–metal systems, and they are undoubtedly very reliable. This suggests that we need to understand the solid mechanics of packed beds if we wish to predict the effective thermal conductivity for unconsolidated systems having large values of k_σ/k_β.

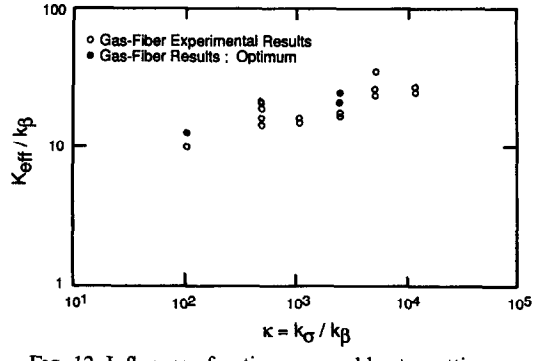

FIG. 12. Influence of optimum guard heater settings.

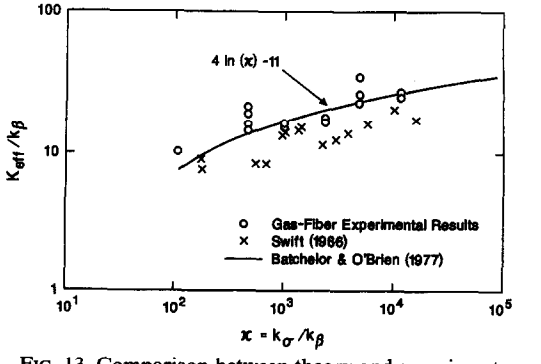

FIG. 13. Comparison between theory and experiment.

CONCLUSIONS

The effective thermal conductivity of a point-contact porous medium has been measured using a unit cell of a spatially periodic porous medium. Significant experimental error is caused by non-uniform heat flow and the presence of natural convection. Nevertheless, the results are in good agreement with the inner expansion theory of Batchelor and O'Brien.

Acknowledgement—This work was supported by NSF grant CPE83-08461.

REFERENCES

1. G. R. Hadley, Thermal conductivity of packed metal powders, *Int. J. Heat Mass Transfer* **29**, 909–920 (1986).
2. S. Whitaker, Simultaneous heat, mass, and momentum transfer : a theory of drying. In *Advances in Heat Transfer*, Vol. 13, pp. 119–203. Academic Press, New York (1977).
3. S. Whitaker, Heat conduction in porous media with homogeneous and heterogeneous thermal sources, *Proceedings Euromech*, Nancy, France, Vol. 194, pp. 39–44 (1985).
4. R. G. Carbonell and S. Whitaker, Heat and mass transfer in porous media. In *Fundamentals of Transport Phenomena in Porous Media* (Edited by J. Bear and M. Y. Corapcioglu), pp. 123–198. Martinus Nijhoff, Dordrecht, The Netherlands (1984).
5. I. Nozad, R. G. Carbonell and S. Whitaker, Heat conduction in multiphase systems I: Theory and experiments for two-phase system, *Chem. Engng Sci.* **40**, 843–855 (1985).
6. S. Whitaker, Heat and mass transfer in granular porous media. In *Advances in Drying*, Vol. 1, pp. 23–61. Hemisphere, New York (1980).
7. H. Brenner, Dispersion resulting from flow through spatially periodic porous media, *Trans. R. Soc. Lond.* **297**, 81–133 (1980).
8. R. C. McPhedran and D. R. McKenzie, The con-

ductivity of lattices of spheres I: The simple cubic lattice, *Proc. R. Soc. Lond.* **A359,** 45–63 (1978).
9. D. R. McKenzie, R. C. McPhedran and G. H. Derrick, The conductivity of lattices of spheres II: The body-centered and face-centered cubic lattices, *Proc. R. Soc. Lond.* **A362,** 211–232 (1978).
10. W. T. Perrins, D. R. McKenzie and R. C. McPhedran, Transport properties of regular arrays of cylinders, *Proc. R. Soc. Lond.* **A369,** 207–225 (1979).
11. A. S. Sangani and A. Acrivos, The effective conductivity of a periodic array of spheres, *Proc. R. Soc. Lond.* **A386,** 263–275 (1983).
12. T.-S. Jiang, M. H. Kim, V. J. Kremesec and J. C. Slattery, The local volume-averaged equations of motion for a suspension of non-neutrally buoyant spheres, *Chem. Engng Commun.* **50,** 1–30 (1987).
13. A. Bensonssan, J. L. Lions and G. Papanicolaou, *Asymptotic Analysis for Periodic Structures.* North-Holland, New York (1978).
14. H.-C. Chang, Multiscale analysis of effective transport in periodic heterogeneous media, *Chem. Engng Commun.* **15,** 83–91 (1982).
15. Y. Ogniewicz and M. M. Yovanovich, Effective conductivity of regularly packed spheres: Basic cell model with constriction. In *Progress in Astronautics and Aeronautics: Heat Transfer and Thermal Control Systems* (Edited by L. S. Fletcher), Vol. 60, pp. 209–228. American Institute of Aeronautics and Astronautics, New York (1978).
16. I. Nozad, An experimental and theoretical study of heat conduction in two- and three-phase systems, Ph.D. thesis, Department of Chemical Engineering, University of California at Davis (1983).
17. J. Oppio, Personal communication (1984). The calculated results for K_{eff}/k_β are available in: S. Whitaker, Heat transfer in catalytic packed bed reactors. In *Handbook of Heat and Mass Transfer.* Vol. III, Chap. 10. Gulf, Houston, Texas (1988).
18. L. C. Wu, Personal communications (1984).
19. G. K. Batchelor and R. W. O'Brien, Thermal or electrical conduction through a granular material, *Proc. R. Soc. Lond.* **A355,** 313–333 (1977).
20. D. R. Shonnard, Experimental determinations of unit cell effective thermal conductivities for point contact, M.S. thesis, Department of Chemical Engineering, University of California at Davis (1985).
21. D. Fournier and S. Klarsfeld, Some recent experimental data on glass fiber insulating materials and their use for a reliable design of insulation at low temperatures. In *Heat Transfer Measurements in Thermal Insulation,* ASTM STP 544, pp. 223–242. Am. Soc. Testing Mater. (1974).
22. R. E. Powe, J. A. Scanlon and E. H. Bishop, Natural convection heat transfer between concentric spheres, *Int. J. Heat Mass Transfer* **13,** 1857–1872 (1970).
23. D. L. Swift, The thermal conductivity of spherical metal powders including the effect of an oxide coating, *Int. J. Heat Mass Transfer* **9,** 1061–1074 (1966).

LA CONDUCTIVITE THERMIQUE EFFECTIVE POUR UN MILIEU POREUX A POINT DE CONTACT: ETUDE EXPERIMENTALE

Résumé—Pour vérifier la théorie de Batchelor et O'Brien pour un milieu poreux à point de contact, est construite une cellule avec un milieu poreux spatialement périodique qui est utilisée pour mesurer la conductivité thermique effective. Cette cellule est constituée d'hémisphères métalliques qui sont amenées à un contact ponctuel déterminé par un brusque changement de conductivité électrique du système. Les données expériementales sont obtenues pour des rapports de conductivitiés thermiques k_σ/k_β allant de 10^2 à 10^4 et les résultats vérifient la dépendance fonctionnelle de K_{eff} vis-à-vis de k_σ/k_β prédite par Batchelor et O'Brien. En outre, les expériences et la théorie de Batchelor et O'Brien sont en bon accord avec les résultats expérimentaux de Swift pour les poudres métalliques ayant des diamètres de particule de l'ordre de quelques centaines de micromètres.

DIE EFFEKTIVE WÄRMELEITFÄHIGKEIT VON PORÖSEN STOFFEN MIT PUNKTKONTAKT: EINE EXPERIMENTELLE UNTERSUCHUNG

Zusammenfassung—Um die Theorie der inneren Expansion von Batchelor und O'Brien für einen porösen Stoff mit Punktkontakt zu überprüfen, wurde eine Einheits-Zelle aus einem räumlich periodisch porösen Stoff konstruiert und für die Messung der effektiven Wärmeleitfähigkeit benutzt. Die Einheits-Zelle besteht aus großen metallischen Halbkugeln, die sich punktförmig berühren, was aufgrund der sprunghaften Änderung der elektrischen Leitfähigkeit des Systems überprüft wurde. Es wurden experimentelle Ergebnisse für einen Bereich des Wärmeleitfähigkeitsverhältnisses k_σ/k_β von 10^2 bis 10^4 ermittelt; diese Ergebnisse bestätigen die nach Batchelor und O'Brien berechnete Abhängigkeit der effektiven Wärmeleitfähigkeit K_{eff} von k_σ/k_β. Darüber hinaus stimmen unsere experimentellen Daten und die theoretischen Ergebnisse nach Batchelor und O'Brien gut mit den Versuchsergebnissen von Swift für Metall-Pulver mit einer Korngröße von mehreren hundert μm überein.

ЭКСПЕРИМЕНТАЛЬНОЕ ИССЛЕДОВАНИЕ ЭФФЕКТИВНОЙ ТЕПЛОПРОВОДНОСТИ ПОРИСТОЙ СРЕДЫ ПРИ ТОЧЕЧНОМ КОНТАКТЕ ЕЕ СТРУКТУРНЫХ ЭЛЕМЕНТОВ

Аннотация—Для проверки теории Батчелора и О'Брайена применительно к пористой среде при точечном контакте ее структурных элементов построена и использована для измерения эффективной теплопроводности элементарная ячейка пространственно периодической пористой среды. Элементарная ячейка выполнена из металлических полусфер большого размера, приведение которых в контакт определяется по резкому изменению электропроводности системы. Получены экспериментальные данные для отношений теплопроводностей k_σ/k_β в диапазоне от 10^2 до 10^4. Результаты подтверждают функциональную зависимость K_{eff} от k_σ/k_β, предсказываемую теорией Батчелора и О'Брайена. Полученные в настоящей работе экспериментальные данные и теория Батчелора хорошо согласуются с экспериментальными результатами Свифта для металлических порошков с диаметрами частиц порядка сотен микрометров.